Vagus nerve stimulation activates two distinct neuroimmune circuits converging in the spleen to protect mice from kidney injury

Shinji Tanaka[a], Chikara Abe[b], Stephen B. G. Abbott[c], Shuqiu Zheng[a], Yusuke Yamaoka[b], Jonathan E. Lipsey[a], Nataliya I. Skrypnyk[a], Junlan Yao[a], Tsuyoshi Inoue[d], William T. Nash[a], Daniel S. Stornetta[c], Diane L. Rosin[c], Ruth L. Stornetta[c], Patrice G. Guyenet[c], and Mark D. Okusa[a,1]

[a]Division of Nephrology and Center for Immunity, Inflammation, and Regenerative Medicine, University of Virginia, Charlottesville, VA 22908; [b]Department of Physiology, Gifu University Graduate School of Medicine, Gifu 501-1194, Japan; [c]Department of Pharmacology, University of Virginia, Charlottesville, VA 22908; and [d]Division of Chronic Kidney Disease Pathophysiology, The University of Tokyo Graduate School of Medicine, Tokyo 113-0033, Japan

Acute kidney injury is highly prevalent and associated with high morbidity and mortality, and there are no approved drugs for its prevention and treatment. Vagus nerve stimulation (VNS) alleviates inflammatory diseases including kidney disease; however, neural circuits involved in VNS-induced tissue protection remain poorly understood. The vagus nerve, a heterogeneous group of neural fibers, innervates numerous organs. VNS broadly stimulates these fibers without specificity. We used optogenetics to selectively stimulate vagus efferent or afferent fibers. Anterograde efferent fiber stimulation or anterograde (centripetal) sensory afferent fiber stimulation both conferred kidney protection from ischemia–reperfusion injury. We identified the C1 neurons–sympathetic nervous system–splenic nerve–spleen–kidney axis as the downstream pathway of vagus afferent fiber stimulation. Our study provides a map of the neural circuits important for kidney protection induced by VNS, which is critical for the safe and effective clinical application of VNS for protection from acute kidney injury.

acute kidney injury | vagus nerve stimulation | sympathetic nervous system | neuroimmune interactions

Acute kidney injury (AKI) is characterized by a rapid loss of kidney function that is indicated by increased serum creatinine and/or decreased urine output. This debilitating condition affects ~10 to 15% of patients admitted to hospitals, and its incidence in intensive care units can exceed 50% (1). AKI is associated with high morbidity and mortality as well as major complications including fluid overload, electrolyte disturbances, uremic complications, and drug toxicity (2). Recent epidemiological and experimental observations have also demonstrated that AKI can lead to chronic kidney disease and kidney failure (3, 4), conditions associated with a lower health–related quality of life and with an increased risk of mortality and cardiovascular morbidity (5, 6). Despite these severe consequences, there are no Food and Drug Administration–approved drugs for the prevention and treatment of AKI. Novel therapies with innovative approaches are desperately needed to address this growing concern.

Mechanisms of neuroimmune regulation have been attracting significant attention for their potential to benefit patients with inflammatory disease (7, 8). Activation of the cholinergic anti-inflammatory pathway (CAP) by vagus nerve stimulation (VNS) is one of the most promising strategies to harness neuroimmune interactions and attenuate inflammation associated with various diseases including kidney disease (9). The vagus nerve (10th cranial nerve) is a bilateral nerve bundle composed of axons of efferent (motor) and afferent (sensory) neurons; the former provides input to thoracic/abdominal organs, and the latter transmits sensory information from these organs to the central nervous system (CNS). The canonical CAP is elicited by the activation of the parasympathetic efferent vagus nerve and requires the spleen; the parasympathetic signal is thought to activate splenic ganglionic noradrenergic neurons

(10) via synapses located within the celiac/suprarenal/superior mesenteric ganglia (11–15). Norepinephrine is released from splenic nerve terminals and binds to β_2 adrenergic receptors expressed on a population of choline acetyltransferase (ChaT)–positive $CD4^+$ $CD44^{high}$ $CD62L^{low}$ memory T cells. This leads to the release of acetylcholine from these cells (16) that binds to $\alpha7$ nicotinic acetylcholine receptors ($\alpha7$nAChRs) expressed on macrophages, resulting in the suppressed production of proinflammatory cytokines (e.g., tumor necrosis factor-α) by macrophages and suppressed inflammation (10, 17). Although activation of this canonical CAP (efferent vagus nerve–splenic nerve–spleen axis) is effective in reducing the severity of many inflammatory disease models, including endotoxemia (10, 16, 17) and colitis (18), other pathways elicited by VNS have also been shown to have an anti-inflammatory effect. For example, the efferent vagus nerve synapses on cholinergic myenteric neurons that are in close contact with muscularis macrophages expressing $\alpha7$nAChRs in the intestine, and VNS activates these macrophages to ameliorate surgery-induced intestinal inflammation (19). Interestingly, electrical stimulation of the central end of the transected vagus nerve ("central VNS") also produces an anti-inflammatory effect in experimental arthritis (20) and endotoxemia (21). These findings suggest that VNS can engage multiple neural circuits in a context-dependent manner to attenuate inflammation.

Significance

The ability of vagus nerve stimulation to generate anti-inflammatory and tissue-protective effects has been known for some time. We have made use of cutting-edge tools to precisely map the neural circuits that contribute to beneficial effects of vagus nerve stimulation. Stimulation was specifically restricted to either the afferent or efferent neurons in the vagus nerve by genetically programming the appropriate cells to express a light-sensitive cation channel. We show that, while both afferent and efferent signals provide protection from kidney injury, afferent stimulation generates a sympathetic response that protects mice in the absence of efferent vagus signals. This provides an insight into the pathways of neuroimmune protection and potential therapeutics.

MEDICAL SCIENCES

www.manaraa.com

VNS was also shown to be effective in kidney transplantation. VNS in brain-dead donor rats reduced inflammation in the donors and immune cell infiltration in the transplanted kidneys in recipients, leading to improved long-term transplant kidney function and recipient survival (22, 23). We previously demonstrated that electrical stimulation of the cervical vagus nerve in mice 24 h before kidney ischemia–reperfusion injury (IRI) markedly attenuated AKI and that the kidney protection was through $\alpha7nAChR^+$ splenocytes (24). However, the precise neural circuit(s) involved in the spleen-dependent kidney protection by VNS remain unknown to date. When the vagus nerve is electrically stimulated, action potentials are transmitted in two directions (anterograde and retrograde) in both efferent and afferent fibers (*SI Appendix*, Fig. S1A): 1) Anterograde efferent fiber stimulation provides input to thoracic/abdominal organs and elicits the canonical CAP. 2) In retrograde efferent fiber stimulation, action potentials propagate back to the cell bodies in the medulla oblongata, which could alter the function of vagus efferent neurons. 3) Anterograde activation of vagal sensory afferents stimulates first-order neurons located in the nucleus tractus solitarius (NTS) and subsequently countless brain regions (25, 26). 4) Retrograde afferent fiber stimulation causes the release of a variety of neuropeptides (e.g., substance P, calcitonin gene-related peptide [CGRP]) at nerve terminals in thoracic/abdominal organs and those peptides have proinflammatory or anti-inflammatory effects on immune cells (27). The neuropeptide release at nerve terminals of afferent sensory neurons may contribute to the development of inflammatory diseases especially in the skin (e.g., psoriasis) (28). On the other hand, release of CGRP from vagal and somatic sensory afferents has direct anti-inflammatory effects on immune cells in the lung and skin (29–31). Thus, retrograde vagal afferent fiber stimulation could contribute to anti-inflammation and organ protection by VNS, a concept that has not previously been explored, due in part to prior methodological constraints. For example, transecting or applying a local anesthetic to the vagus nerve to block nerve conduction prior to electrical stimulation enables a distinction between distal and central VNS effects, but this strategy is still not selective because VNS elicits a combination of anterograde and retrograde stimulation in efferent and afferent fibers in this setting (*SI Appendix*, Fig. S1B).

As a first step to identify the neural circuit(s) involved in the kidney protection by VNS, we utilized optogenetics for selective stimulation of vagus efferent or afferent fibers and demonstrated that anterograde stimulation of either efferent or afferent fibers is sufficient to protect the kidneys from IRI. We also showed that the protection is mediated by splenocytes in both cases. Since the protective effect of anterograde efferent fiber stimulation is consistent with the CAP activation, we further sought to identify the downstream pathway of anterograde afferent fiber stimulation. Vagal sensory afferents innervate the NTS, which projects in turn to many other regions in the CNS (32). We explored three downstream pathways to the periphery: 1) vagal efferents (a vagovagal reflex), 2) sympathetic efferents (a vagosympathetic reflex), and 3) hypothalamo–pituitary–adrenocortical (HPA) axis, all of which can have immunomodulatory effects upon activation (9, 33, 34), and our findings strongly suggest that a vagosympathetic reflex plays an important role in the kidney protection by vagal afferent fiber stimulation. We further identified the splenic nerve as a critical branch of the sympathetic nerve in mediating kidney protection, which is consistent with the importance of splenocytes in this context.

Next, we sought to identify a central node in the CNS that mediates the vagosympathetic reflex to confer kidney protection. C1 neurons, which reside in the rostral ventrolateral medulla (RVLM), are glutamatergic, catecholaminergic, and peptidergic neurons, and receive direct input from neurons of the NTS (35). The C1 neurons are activated by a variety of physical stressors

and circulating inflammatory molecules and serve as a central regulator of autonomic function (36, 37). They innervate sympathetic preganglionic neurons in the intermediolateral cell column of the spinal cord as well as neurons in the dorsal motor nucleus of the vagus (where most of the neurons of the efferent vagus nerve originate) and neurons in the paraventricular nucleus of the hypothalamus (the primary driver of the HPA axis) (36). We previously demonstrated that selective stimulation of C1 neurons protected the kidneys from AKI (38). Here we demonstrate that C1 neurons are an integrative center for the neural pathway in vagus afferent fiber stimulation and kidney protection. Our study defines a neural circuit involved in kidney protection by VNS, which is critical for the safe and effective clinical application of VNS for protection from AKI.

Results

Anterograde Stimulation of Either Vagal Efferent or Afferent Fibers Is Sufficient to Protect Kidneys Against IRI. To determine the vagus nerve pathways leading to protection of kidneys from IRI we created and validated mice expressing channelrhodopsin-2 (ChR2) in efferent and afferent vagus fibers (for details, see *SI Appendix,* Validation of Mouse Models for Selective Vagus Efferent versus Vagus Afferent Fiber Stimulation). Since Chat and vesicular glutamate transporter 2 (Vglut2) are established markers for vagal efferent and sensory afferent neurons, respectively (26, 39, 40), we crossed heterozygous *Chat-ires-Cre* and *Vglut2-ires-Cre* mice with homozygous *Ai32* mice (containing a Cre-dependent ChR2-enhanced yellow fluorescent protein [eYFP] allele) to produce *Chat-ChR2* mice (for selective optogenetic efferent fiber stimulation), *Vglut2-ChR2* mice (for selective optogenetic afferent fiber stimulation), and littermate controls (*SI Appendix,* Fig. S2). Using histological methods, we confirmed that, within the vagus nerve, ChR2 is selectively expressed in efferent fibers in *Chat-ChR2* mice and in sensory afferents in *Vglut2-ChR2* mice (*SI Appendix,* Fig. S3 A–N). We also verified that application of blue laser light to the cervical vagus nerve of *Chat-ChR2* and *Vglut2-ChR2* mice evoked propagated action potentials (*SI Appendix,* Fig. S4 A–C). Finally, we showed that optical activation of vagal ChR2+ fibers produced physiological responses consistent with the selective activation of vagal efferents in *Chat-ChR2* mice and the selective activation of vagal afferents in *Vglut2-ChR2* mice (*SI Appendix,* Figs. S5 A–F and S6 A–D). A 5 Hz stimulation frequency was used to investigate the protective effect of optogenetic VNS against kidney injury; this stimulation produced a small (<10%) but reliable reduction in heart rate and respiratory rate (*SI Appendix,* Fig. S5 C and D).

We previously showed that electrical stimulation of the left cervical vagus nerve protected the kidneys against IRI (an established mouse model of AKI) (24). Electrical VNS activates four distinct neural pathways: efferent and afferent fibers in anterograde and retrograde directions (*SI Appendix,* Fig. S1A). To identify which pathway is critical to protect the kidneys, we applied blue laser light to the left cervical vagus nerve of *Chat-ChR2* and *Vglut2-ChR2* mice (optogenetic VNS) 24 h before bilateral kidney IRI (26 min of kidney ischemia followed by reperfusion). Mice were euthanized after 24 h of kidney reperfusion (Fig. 1A). Optogenetic VNS in *Chat-ChR2* mice (Fig. 1B) significantly attenuated the increase in plasma creatinine (a plasma marker for renal function) following injury (Fig. 1C), histologically detectable tubular injury (Fig. 1D and *SI Appendix,* Fig. S7A), renal *Havcr1* (Kim-1, a marker for tubular injury) expression (Fig. 1E), neutrophil infiltration (*SI Appendix,* Fig. S7B), and renal inflammatory cytokine/chemokine expression (*SI Appendix,* Fig. S7C), showing that vagus efferent fiber stimulation in an anterograde and/or retrograde manner ameliorates kidney IRI. Ameliorated kidney injury by vagus efferent fiber stimulation was accompanied by reduced circulating inflammatory cytokine concentrations (*SI Appendix,* Fig. S7D). To identify whether the protection was caused by the retrograde or
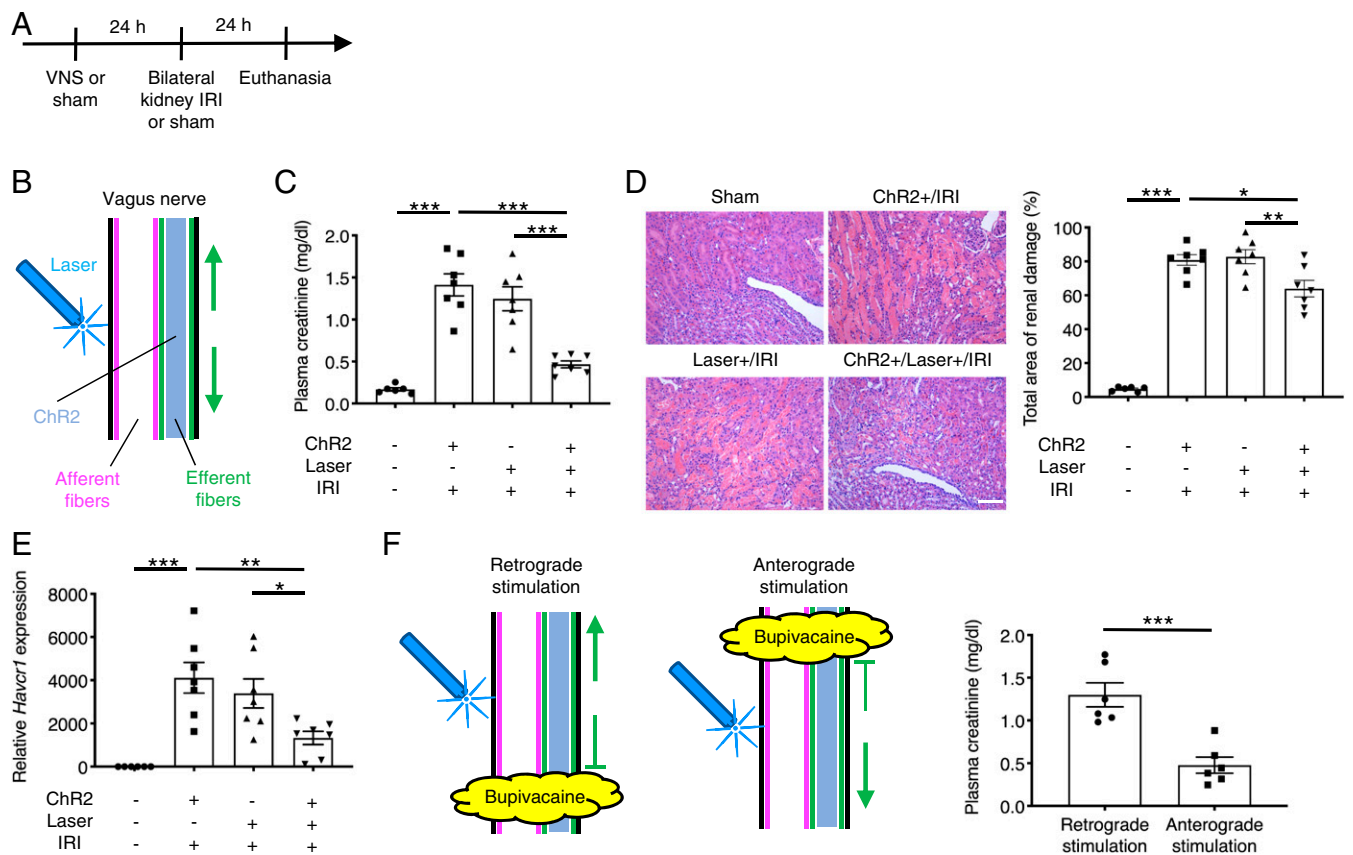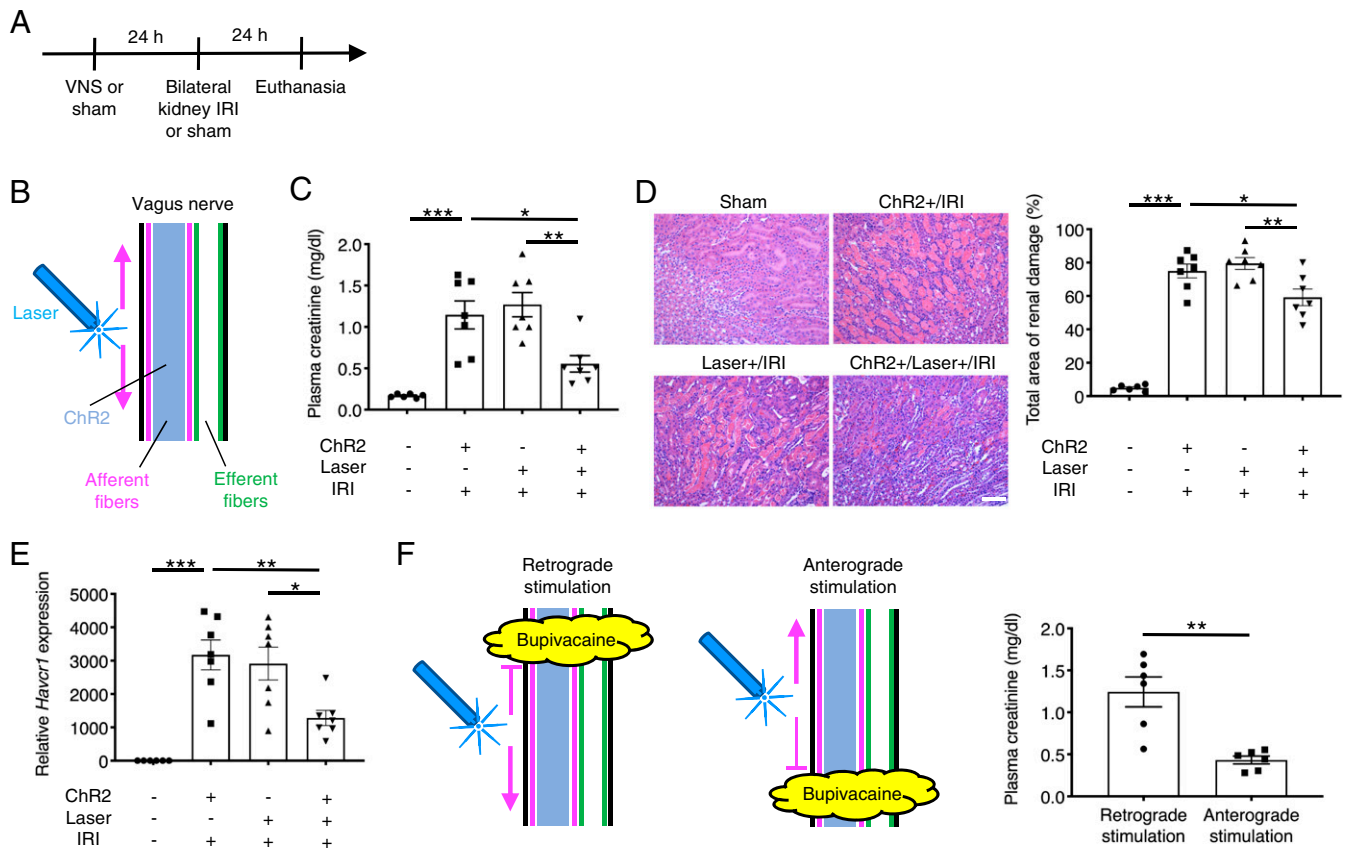
Fig. 1. Optogenetic stimulation of vagus efferent fibers in an anterograde direction protects kidneys against IRI. (*A*) Timeline of experiments. (*B*) Illustration depicting optogenetic stimulation of cervical vagus nerve in *Chat-ChR2* mice. Note that action potentials elicited in response to optogenetic stimulation are transmitted only in efferent fibers in both anterograde (downward arrow; toward the periphery) and retrograde (upward arrow; toward the brain) directions. Blue shading, fibers that express ChR2 and that can be activated by blue laser. (*C–E*) Effect of selective efferent fiber stimulation (5 Hz, 10 min) on plasma creatinine (a representative marker for kidney function) (*C*), acute tubular necrosis score (% of total surface area of the kidney section occupied by tubule injury) with representative hematoxylin and eosin (H&E) staining in outer medulla of kidney sections (*D*), and renal *Havcr1* (Kim-1, a representative marker for tubular injury) mRNA (*E*) in *Chat-ChR2* and control mice. (*F*) Effect of optogenetic retrograde versus anterograde efferent vagus nerve fiber stimulation (5 Hz, 10 min) on plasma creatinine in *Chat-ChR2* mice with illustration depicting the strategy. Blue laser was applied to the central (for retrograde stimulation) or distal (for anterograde stimulation) side of the area anesthetized with bupivacaine. $n = 6$ in sham IRI group and $n = 7$ in IRI groups (*C–E*); $n = 6$ in each group in bupivacaine experiments (*F*). Scale bar, 100 μm. Data are represented as mean ± SEM; *$P < 0.05$, **$P < 0.01$, and ***$P < 0.001$ by one-way ANOVA with post hoc Tukey test (*C–E*) or unpaired two-sided Student's *t* test (*F*).

anterograde activation of cholinergic vagal axons, we applied bupivacaine (a local anesthetic) directly to the vagus nerve to block nerve conduction and then applied blue laser to the central (for retrograde stimulation) or distal (for anterograde stimulation) side of the anesthetized area (Fig. 1*F*). Plasma creatinine data showed that anterograde but not retrograde stimulation of efferent fibers was protective against kidney IRI (Fig. 1*F*). We performed similar experiments using *Vglut2-ChR2* mice to investigate the role of afferent fibers in the kidney protection by VNS (Fig. 2 *A–F*). Interestingly, selective vagus afferent fiber stimulation (Fig. 2*B*) also significantly decreased plasma creatinine (Fig. 2*C*), histological tubular injury (Fig. 2*D* and *SI Appendix*, Fig. S8*A*), renal *Havcr1* expression (Fig. 2*E*), neutrophil infiltration (*SI Appendix*, Fig. S8*B*), and renal inflammatory cytokine/chemokine expression (*SI Appendix*, Fig. S8*C*) 24 h after kidney IRI. Ameliorated kidney injury by vagus afferent fiber stimulation was accompanied by reduced circulating inflammatory cytokine concentrations (*SI Appendix*, Fig. S8*D*). Next, we tested whether retrograde stimulation of afferent vagus nerve fibers could contribute to anti-inflammation and kidney protection, perhaps through the peripheral release of neuropeptides. Nerve conduction blockade by bupivacaine application caudal or

cephalad to the site where laser light was applied to the vagal nerve revealed that anterograde but not retrograde stimulation of afferent fibers was protective against kidney IRI (Fig. 2*F*). Taken together, these findings suggest that two distinct neural pathways (anterograde efferent and anterograde afferent fiber stimulation) contribute to the protective effect of electrical VNS against kidney IRI.

Kidney Protection by Vagus Efferent and Afferent Fiber Stimulation Is Mediated by Splenocytes. We previously demonstrated that kidney protection by whole nerve electrical VNS is mediated by splenocytes (24). However, it is currently unknown if protection by both vagus efferent and afferent fiber stimulation is also specifically via effects on splenocytes. To address this question, splenectomy was performed seven days before vagus efferent or vagus afferent fiber stimulation (Fig. 3 *A–C*). In splenectomized mice, neither form of stimulation was protective against kidney IRI, suggesting that splenocytes are necessary for the protection in both cases. Next, we performed adoptive transfer experiments (Fig. 3 *D–F* and *SI Appendix*, Fig. S9 *A* and *B*). Donor mice underwent vagus efferent or afferent fiber stimulation or sham stimulation, and 24 h later, splenocytes were isolated from the donor mice and were injected

Tanaka et al.
Vagus nerve stimulation activates two distinct neuroimmune circuits converging in the spleen to protect mice from kidney injury

PNAS | 3 of 12
https://doi.org/10.1073/pnas.2021758118

MEDICAL SCIENCES

Fig. 2. Optogenetic stimulation of vagus afferent fibers in an anterograde direction protects kidneys against IRI. (*A*) Timeline of experiments. (*B*) Illustration depicting optogenetic stimulation of cervical vagus nerve in *Vglut2-ChR2* mice. Note that action potentials elicited in response to optogenetic stimulation are transmitted only in afferent fibers in both anterograde (upward arrow; toward the brain) and retrograde (downward arrow; toward the periphery) directions. Blue shading, fibers that express ChR2 and that can be activated by blue laser. (*C–E*) Effect of selective afferent fiber stimulation (5 Hz, 10 min) on plasma creatinine (*C*), acute tubular necrosis score (% of total surface area of the kidney section occupied by tubule injury) with representative H&E staining in outer medulla of kidney sections (*D*), and renal *Havcr1* mRNA (*E*) in *Vglut2-ChR2* and control mice. (*F*) Effect of optogenetic retrograde versus anterograde afferent vagus nerve fiber stimulation (5 Hz, 10 min) on plasma creatinine in *Vglut2-ChR2* mice with illustration depicting the strategy. Blue laser was applied to the distal (for retrograde stimulation) or central (for anterograde stimulation) side of the area anesthetized with bupivacaine. $n = 6$ in sham IRI group and $n = 7$ in IRI groups (*C–E*); $n = 6$ in each group in bupivacaine experiments (*F*). Scale bar, 100 μm. Data are represented as mean ± SEM; *$P < 0.05$, **$P < 0.01$, and ***$P < 0.001$ by one-way ANOVA with post hoc Tukey test (*C–E*) or unpaired two-sided Student's t test (*F*).

intravenously (i.v.) (1×10^6 cells/recipient mouse) into naïve recipient wild-type mice. The recipient mice were then subjected to kidney IRI 24 h after splenocyte transfer. Adoptive transfer of splenocytes from mice that underwent either vagus efferent or afferent fiber stimulation protected recipient mice from kidney IRI, which was accompanied by reduced circulating inflammatory cytokine concentrations, while splenocytes from sham stimulation donors were not protective (Fig. 3 *E* and *F* and *SI Appendix*, Fig. S9 *A* and *B*). These results suggest that splenocytes are necessary and sufficient for the kidney protection elicited by either vagus efferent or vagus afferent fiber stimulation. We also performed adoptive transfer experiments using lymph node cells and bone marrow cells isolated from donor mice that underwent sham VNS or electrical VNS (*SI Appendix*, Fig. S10*A*) to investigate whether these cells contribute to the protective effect of VNS possibly through recruitment to the spleen. Adoptive transfer of lymph node cells (*SI Appendix*, Fig. S10*B*) or bone marrow cells (*SI Appendix*, Fig. S10*C*) did not confer protection. This result further supports a critical role of spleen/splenocytes in this context.

Vagus Afferent Fiber Stimulation Protects the Kidney Against IRI by Activating a Vagosympathetic Splenic Reflex. Both vagus efferent and afferent fiber stimulation affected splenocytes, which contributed to

kidney protection (Fig. 3 *A–F*). The effectiveness of vagus efferent fiber stimulation is consistent with the canonical CAP in which vagus efferent fibers, splenic nerve, and splenocytes play critical roles to exert an anti-inflammatory effect (9, 10, 16, 17). The effect of vagus afferent fiber stimulation could also be explained by the canonical CAP since vagal afferent stimulation can elicit a vago-vagal reflex (41). However, vagal afferent stimulation also elicits a vagosympathetic reflex (42), which could confer protection against AKI by activating the sympathetic innervation of the spleen. Finally, vagal afferent stimulation could protect from AKI by activating the HPA axis and enhancing the release of corticosterone [the principal glucocorticoid in mice (43)].

To investigate whether the HPA axis is activated by vagus afferent fiber stimulation, we examined plasma corticosterone levels just after stimulation (Fig. 4*A*). Plasma corticosterone concentration was significantly increased after selective anterograde vagus afferent fiber stimulation in *Vglut2-ChR2* mice, indicating that the HPA axis is indeed activated by vagus afferent fiber stimulation. However, the protective effect was not abolished by blocking corticosterone receptors with mifepristone (Fig. 4 *B* and *C*). Next, we tested whether the protection against AKI elicited by vagal afferent fiber stimulation could be the result of the CAP via a vagovagal reflex. The results were negative; the protective effect of
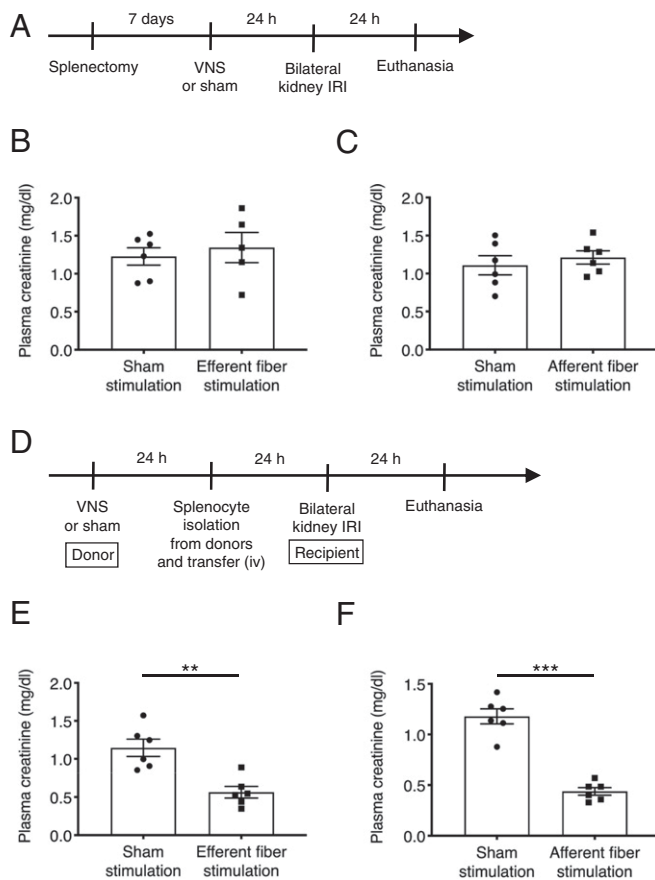
Fig. 3. A critical role of splenocytes in the protective effect of vagus efferent and afferent fiber stimulation against kidney IRI. (*A*) Timeline of experiments for *B* and *C*. (*B* and *C*) Plasma creatinine 24 h after bilateral kidney IRI. Mice underwent optogenetic vagus efferent fiber stimulation (*Chat-ChR2* mice, *B*), afferent fiber stimulation (*Vglut2-ChR2* mice, *C*), or sham stimulation (same trains of laser light delivered to Cre-negative littermates, *B* and *C*) 7 d after splenectomy. (*D*) Timeline of experiments for *E* and *F*. (*E* and *F*) Plasma creatinine 24 h after bilateral kidney IRI. Donor mice underwent optogenetic vagus efferent fiber stimulation (*Chat-ChR2* mice, *E*), afferent fiber stimulation (*Vglut2-ChR2* mice, *F*), or sham stimulation (same trains of laser light delivered to Cre-negative littermates, *E* and *F*), and 24 h later, splenocytes were isolated from the donor mice and were injected i.v. (1 × 10^6 cells/recipient mouse) into naïve recipient wild-type mice. The recipient mice were subjected to kidney IRI 24 h after splenocyte transfer. $n = 6$ in each group (*B*, *C*, *E*, *F*) except for the efferent fiber stimulation group in the splenectomy experiment ($n = 5$, *B*). Data are represented as mean ± SEM; **$P <$ 0.01 and ***$P <$ 0.001 by unpaired two-sided Student's *t* test (*B*, *C*, *E*, *F*).
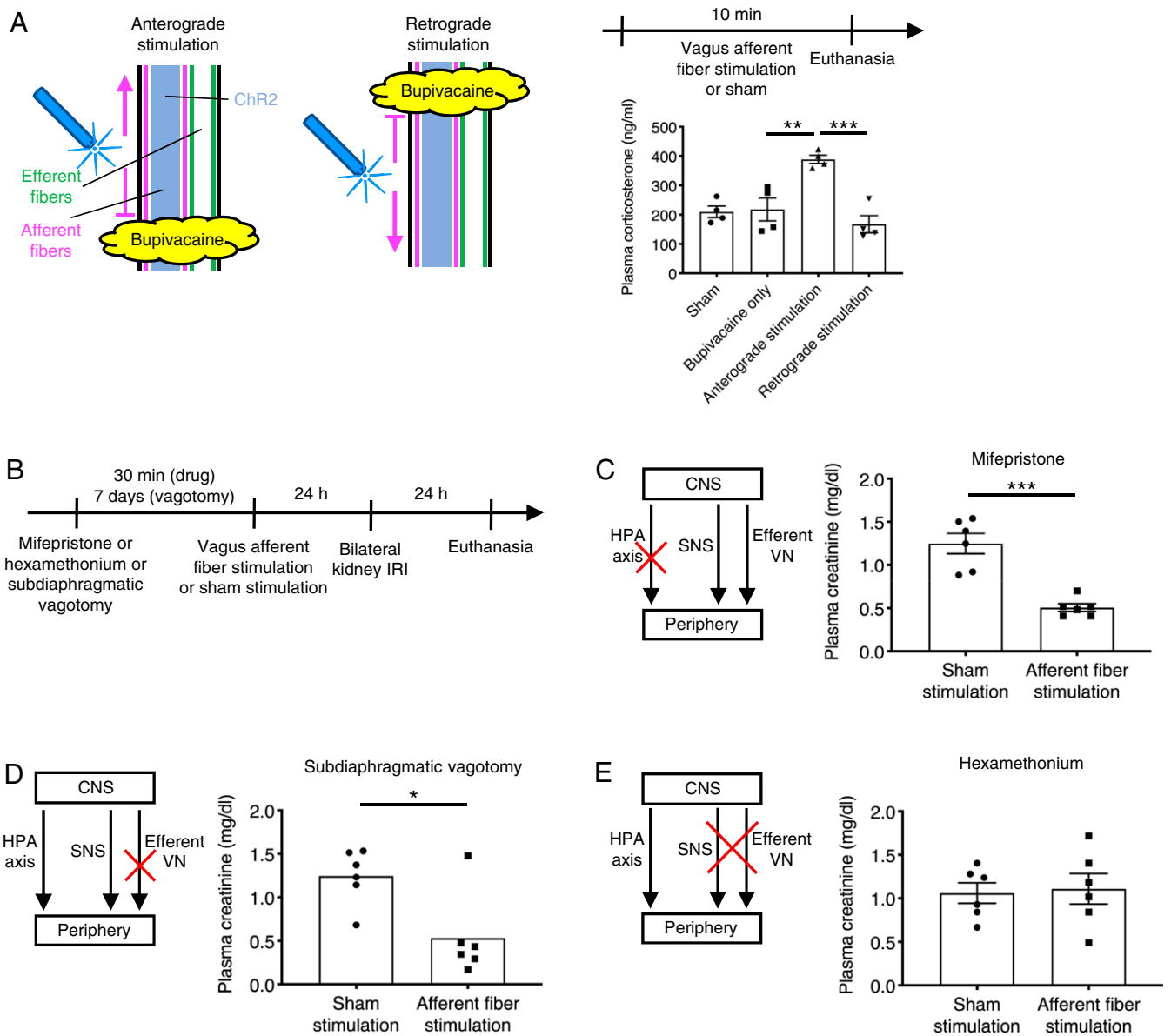
vagal afferent stimulation persisted after subdiaphragmatic vagotomy (Fig. 4*D*; the efficacy of the vagotomy is shown in *SI Appendix*, Fig. S11). These negative results suggested that vagal afferent stimulation could protect the kidneys from AKI via a vagosympathetic reflex. The following experiments were designed to test this hypothesis and to determine which sympathetic nerve (to the adrenal medulla, the kidneys, and the spleen) played the most critical role.

First, we showed that vagal afferent stimulation produced powerful evoked responses in three sympathetic nerves (splenic, renal, and lumbar) thereby demonstrating that vagal afferent stimulation also activates the sympathetic nervous system (*SI Appendix*, Fig. S12). We used Sprague–Dawley rats in this experiment because of the difficulty to record from these nerves (especially the splenic nerve) in mice. We also confirmed that VNS with the parameters used for nerve recordings (square wave, 5 Hz, 150 μA intensity, and 1 ms pulses) produced protection against kidney IRI in rats (plasma creatinine: 2.30 ± 0.08 mg/dL

[sham VNS, $n = 5$] versus 1.58 ± 0.13 mg/dL [VNS, $n = 5$], $P =$ 0.0020 by unpaired two-sided Student's *t* test). Next, we showed that the protective effect of vagal afferent stimulation in mice was abolished by administering hexamethonium (Fig. 4*E*), a ganglionic blocker that eliminates the activation of the sympathetic and parasympathetic systems. Given that subdiaphragmatic vagotomy was ineffective, this result strongly suggested that a vagosympathetic reflex mediates the renal protection elicited by vagus afferent fiber stimulation. To determine which sympathetic efferent pathways mediate kidney protection induced by vagus afferent fiber stimulation, we conducted a series of ablation studies (Fig. 5 *A* and *B*). In the canonical CAP, norepinephrine locally released from splenic nerve terminals binds to β_2 adrenergic receptors expressed on ChAT-positive T cells in the spleen; however, β_2 receptors have a much higher affinity for epinephrine than for norepinephrine (44). Thus, epinephrine, released from the adrenal medulla into the circulation could be the catecholamine that activates β_2 adrenergic receptors in splenocytes. To test this possibility, we performed adrenalectomy before vagus afferent fiber stimulation, but adrenalectomy did not prevent kidney protection (Fig. 5*C*). Next, we explored the potential contribution of the splenic and renal nerves, which are predominantly sympathetic, to kidney protection by vagus afferent fiber stimulation. Efficacy and selectivity of splenic and renal denervation by local application of 10% phenol were confirmed by diminished tyrosine hydroxylase (TH)–positive nerve fibers in tissue sections of kidney and spleen and significantly reduced norepinephrine in the tissues seven days after denervation surgery (without kidney IRI) (Fig. 5*D*). Splenic denervation eliminated the kidney protection elicited by vagus afferent fiber stimulation (Fig. 5*E*), whereas renal denervation had no effect (Fig. 5*F*). These results strongly suggest that vagus nerve afferent fiber stimulation protects the kidneys from IRI via activation of the splenic nerve by a vagosympathetic reflex.

The C1 Neurons Play a Pivotal Role in the Renoprotective Effect of Vagus Afferent Fiber Stimulation. The C1 neurons, which reside in the RVLM, are activated by stresses such as nociceptive stimuli, inflammation, hypoxia, and hypotension, and they contribute to the autonomic nervous system and HPA responses to these stresses (36). We hypothesized that these neurons also mediate the vagosympathetic reflex that protects the kidneys from IRI. In support of this hypothesis, selective stimulation of C1 neurons protects against kidney IRI, and this protection is dependent on the spleen (38). C1 neurons were indeed activated by vagus afferent fiber stimulation as judged by a significant increase in the percentage of C1 neurons that were c-Fos–positive (Fig. 6*A*). This percentage was unchanged by efferent fiber stimulation, and, as anticipated, the total number of C1 neurons identified was the same in control, *Vglut2-ChR2*, and *Chat-ChR2* mice (387 ± 20, 401 ± 7, and 408 ± 20, respectively). Next, we explored whether C1 neurons are necessary for the kidney protection by vagus afferent fiber stimulation (Fig. 6*B*). To selectively ablate C1 neurons (catecholaminergic neurons that express the catecholamine synthetic enzyme, dopamine β-hydroxylase [DBH]) without affecting other types of neurons, we used genetically engineered caspase-3 that upon activation commits a cell to apoptosis. Caspase vector (AAV2-DIO-taCasp3-TEVp) (45) or control vector (AAV2-DIO-EF1α-mCherry) was microinjected bilaterally into the RVLM of *Dbh-Cre* mice. Within 5 to 6 wk, this procedure resulted in the near complete elimination of C1 neurons in the caspase vector group (Fig. 6*C*). Regarding the specificity of this ablation strategy, we previously demonstrated that all other adrenergic and noradrenergic cell groups outside of the C1 region appeared intact and that the cholinergic neurons comingled with C1 neurons were intact (38). The high selectivity of the control (mCherry-expressing) vector for RVLM catecholaminergic neurons ($TH^+mCherry^+$/total $mCherry^+$: 96.5 ± 0.7%) also suggested a minimal off-target rate of infection by the caspase vector. In the sham, control vector, and C1-ablated groups, we performed "distal

Tanaka et al.
Vagus nerve stimulation activates two distinct neuroimmune circuits converging in the spleen to protect mice from kidney injury

PNAS | 5 of 12
https://doi.org/10.1073/pnas.2021758118

Fig. 4. Sympathetic nervous system plays a predominant role in kidney protection by vagus afferent fiber stimulation. (*A*) Plasma corticosterone levels immediately after vagus afferent fiber stimulation or sham stimulation (by setting the laser output to zero) for 10 min in *Vglut2-ChR2* mice with illustration depicting optogenetic anterograde versus retrograde VNS. Bupivacaine was directly applied to the left cervical vagus nerve to block nerve conduction, and blue laser was applied to the central or distal side of the anesthetized area for anterograde or retrograde stimulation, respectively. (*B*) Timeline of experiments (*C–E*) for investigating which pathway among HPA axis, sympathetic nervous system (SNS), and efferent vagus nerve (VN) mediates the protective effect of vagus afferent fiber stimulation against kidney IRI. (*C–E*) Plasma creatinine 24 h after bilateral kidney IRI. Mice were given mifepristone (corticosterone receptor antagonist, *C*) or hexamethonium (ganglionic blocker, *E*) or underwent subdiaphragmatic vagotomy (*D*) before optogenetic vagus afferent fiber stimulation (*Vglut2-ChR2* mice) or sham stimulation (same trains of laser light delivered to Cre-negative littermates). $n = 4$ in each group (*A*), and $n = 6$ in each group (*C–E*). Data are represented as mean $\pm$ SEM. When no error bar is shown, this is because the data were not normally distributed, and a nonparametric test was used. *$P < 0.05$, **$P < 0.01$, and ***$P < 0.001$ by one-way ANOVA with post hoc Tukey test (*A*), unpaired two-sided Student's *t* test (*C* and *E*), or two-sided Mann–Whitney test (*D*). CNS, central nervous system.

VNS" or "central VNS" in which electrodes were positioned at the distal or central side of the area anesthetized with bupivacaine in the left cervical vagus nerve, 24 h prior to bilateral kidney IRI (Fig. 6*B*). Since retrograde stimulation of each type of fiber did not contribute to kidney protection (Figs. 1*F* and 2*F*), distal VNS and central VNS are equivalent to anterograde efferent and afferent fiber stimulation, respectively. Both distal VNS and central VNS were protective against kidney IRI in the sham group and control vector group, and control vector injection did not affect the extent of kidney injury (Fig. 6*D*). In contrast, in the caspase vector group, distal VNS was protective whereas central VNS was ineffective.

Abrogation of the protection by central VNS against IRI in the caspase group was further confirmed by renal histology (Fig. 6*E*) and renal *Havcr1* expression (Fig. 6*F*). These results indicate that C1 neurons mediate the kidney protection by vagus afferent fiber stimulation, but they are not necessary for the kidney protection elicited by vagus efferent fiber stimulation.
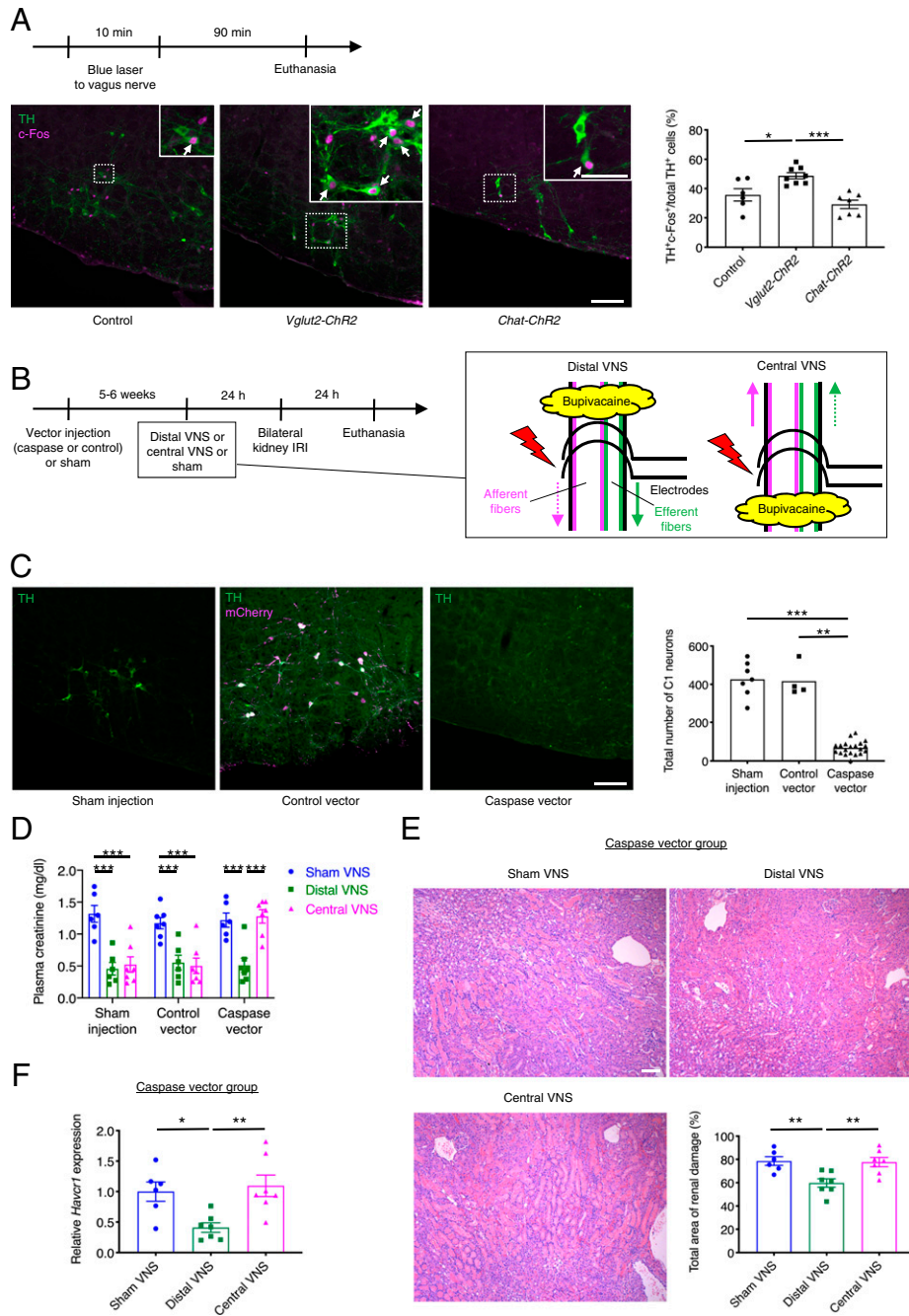
Discussion

VNS is a promising therapeutic option in various diseases as shown in recent clinical studies in patients with rheumatoid arthritis and Crohn's disease (46, 47). Further progress depends on
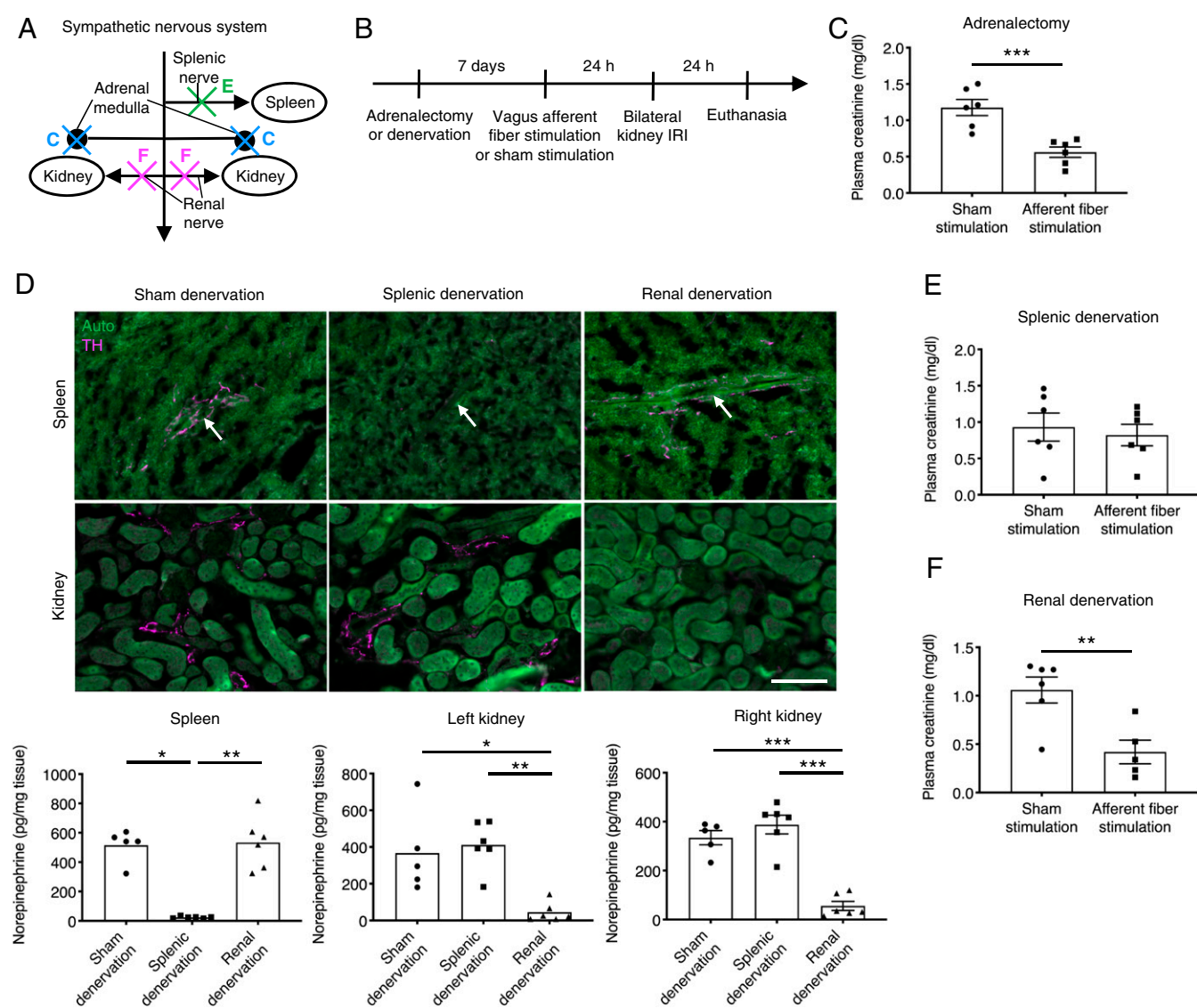
Fig. 5. Splenic nerve mediates the protective effect of vagus afferent fiber stimulation against kidney IRI. (*A*) Illustration depicting ablation studies (*C*–*F*) in the sympathetic nervous system. Adrenalectomy (*C*), splenic denervation (*E*), or renal denervation (*F*) was performed seven days before optogenetic vagus afferent fiber stimulation (*Vglut2-ChR2* mice) or sham stimulation (same trains of laser light delivered to Cre-negative littermates) to investigate components of the sympathetic nervous system that mediate the protective effect of vagus afferent fiber stimulation against kidney IRI. (*B*) Timeline of experiments for *C*, *E*, and *F*. (*C*, *E*, and *F*) Plasma creatinine 24 h after bilateral kidney IRI in mice with adrenalectomy (*C*), splenic denervation (*E*), and renal denervation (*F*). (*D*) Efficacy and selectivity of splenic and renal denervation. Mice were euthanized seven days after splenic denervation, renal denervation, or sham denervation (without kidney IRI). Norepinephrine levels (determined by HPLC) in the spleen and kidneys are shown with representative immunofluorescent labeling of spleen/kidney sections for TH (a marker for sympathetic nerves; magenta). White arrows indicate a branch of the splenic artery, with which sympathetic nerves in the spleen run in parallel. Auto, green autofluorescence in spleen/kidney sections. $n = 6$ in each group (*C* and *E*); Sham denervation: $n = 5$, Splenic denervation: $n = 6$, Renal denervation: $n = 6$ (*D*); Sham stimulation: $n = 6$, Afferent fiber stimulation: $n = 5$ (*F*). (Scale bar, 100 μm.) Data are represented as mean ± SEM. When no error bar is shown, this is because the data were not normally distributed, and a nonparametric test was used. *$P < 0.05$, **$P < 0.01$, and ***$P < 0.001$ by unpaired two-sided Student's *t* test (*C*, *E*, and *F*), Kruskal–Wallis with Dunn's test (*D*, Spleen and Left kidney), or one-way ANOVA with post hoc Tukey test (*D*, Right kidney).

identifying which vagal axons and neural circuits are responsible for the beneficial effects. Electrical stimulation has been used in most of the VNS studies; however, this method has limited ability to identify which neurons (afferent or efferent) are responsible for the beneficial effects and which processes of these neurons (central or peripheral) mediate the observed benefits. A contribution of vagus efferent fibers to anti-inflammation and organ protection by VNS has been suggested because electrical stimulation of the peripheral end of the transected vagus nerve is effective (*SI Appendix*, Fig. S1*B*) (24, 48, 49). However, this method fails to distinguish anterograde efferent fiber stimulation

and retrograde afferent fiber stimulation; the latter potentially has immunomodulatory effects on immune cells in many organs (25–27, 29–31). Using optogenetics for selective stimulation of vagus efferent versus afferent fibers combined with nerve conduction blockade, we demonstrated that either anterograde efferent fiber stimulation or anterograde afferent fiber stimulation protects the kidneys against IRI whereas retrograde activation of these neurons had no effect. Although it is still controversial whether vagal efferent neurons synapse with postganglionic sympathetic neurons supplying the spleen (50–52), this is a direct demonstration that vagus efferent (motor) neurons contribute to

Tanaka et al.
Vagus nerve stimulation activates two distinct neuroimmune circuits converging in the spleen to protect mice from kidney injury

PNAS | 7 of 12
https://doi.org/10.1073/pnas.2021758118
www.manaraa.com

Fig. 6. C1 neurons in the lower brainstem mediate the protective effect of vagus afferent fiber stimulation against kidney IRI. (*A*) Percentage of total C1 neurons (TH$^+$) that are activated (TH$^+$c-Fos$^+$) in Cre-negative littermate controls, *Vglut2-ChR2* (for afferent fiber stimulation), and *Chat-ChR2* (for efferent fiber stimulation) mice with representative images of TH (green, in cytoplasm) and c-Fos (magenta, in nuclei) immunoreactivity in the (coronal plane, −6.7 mm from bregma). Mice were euthanized 90 min after blue laser application to the left cervical vagus nerve. TH and c-Fos immunoreactivities were assessed in the RVLM, where C1 neurons reside. White arrows indicate activated C1 neurons (TH$^+$c-Fos$^+$). (Scale bars: 100 μm; 50 μm (*Inset*). (*B*) Timeline of experiments for *C–F* with illustration depicting distal and central electrical VNS and positioning of electrodes. Caspase 3 vector (AAV2-DIO-taCasp3-TEVp) or control vector (AAV2-DIO-EF1α-mCherry) was microinjected bilaterally to RVLM of *Dbh-Cre* mice 5 to 6 wk prior to electrical (distal or central) VNS (5 Hz, 10 min) to selectively ablate C1 neurons. Electrodes were positioned at the distal or central side of the area anesthetized with bupivacaine in the left cervical vagus nerve. Solid and dotted arrows indicate action potential transmissions in anterograde and retrograde directions in each type of fibers, respectively. (*C*) Total number of C1 neurons assessed by TH immunoreactivity in RVLM with representative images of TH (green) and mCherry (magenta) immunoreactivity in the RVLM (coronal plane, −6.7 mm from bregma). Colocalization of TH and mCherry immunoreactivity is shown in white. (Scale bar, 100 μm.) (*D–F*) Plasma creatinine in all groups (*D*), acute tubular necrosis score (% of total surface area of the kidney section occupied by tubule injury) with representative H&E staining in outer medulla of kidney sections (*E*) and renal *Havcr1* mRNA (*F*) in the caspase vector group 24 h after bilateral kidney IRI. (Scale bar: 100 μm.) Control: n = 6, *Vglut2-ChR2*: n = 8, *Chat-ChR2*: n = 7 (*A*); Sham injection: n = 7, Control vector: n = 4, Caspase vector: n = 20 (*C*); n = 6–7 in each group (*D–F*). Data are represented as mean ± SEM. When no error bar is shown, this is because the data were not normally distributed, and a nonparametric test was used. *$P < 0.05$, **$P < 0.01$, and ***$P < 0.001$ by one-way ANOVA with post hoc Tukey test (*A*, *E*, and *F*), Kruskal–Wallis with Dunn's test (*C*), or two-way ANOVA with post hoc Tukey test (*D*).

www.manaraa.com

organ protection by VNS, which is consistent with the canonical CAP (9). Splenectomy and adoptive transfer data strongly suggest that kidney protection by vagus efferent and afferent fiber stimulation is mediated by splenocytes. However, the mechanism by which splenocytes protect the kidney including potential humoral factors is yet to be determined.

The efficacy of vagal afferent stimulation to reduce AKI implies the existence of a reflex, which we attempted to identify here. We explored three possible pathways: vagal efferents (a vagovagal reflex), sympathetic efferents (a vagosympathetic reflex), and HPA axis. Activation of any one of these outflows could potentially explain the protective effect of vagal afferent stimulation against AKI (9, 33, 34). We previously showed that a brief restraint stress protected the kidneys from IRI through the activation of C1 neurons, which was accompanied by increased plasma corticosterone levels (38). Thus, it is possible that molecules upregulated under stress conditions (e.g., glucocorticoid and catecholamines) play an important role in the protective effect by vagal afferent stimulation. Indeed, glucocorticoid administration ameliorated kidney IRI, which was accompanied by suppressed inflammation including less neutrophil infiltration (53). However, our results strongly suggest that the predominant mechanism is a vagosympathetic reflex that is mediated via the splenic nerve and operates by changing the phenotype of splenocytes (*SI Appendix*, Fig. S13). This is consistent with previous findings that sympathetic nerves rather than the HPA axis mediate anti-inflammatory effects of vagal afferent stimulation in arthritis (20) and endotoxemia (21). Interestingly, subdiaphragmatic vagotomy, which eliminates the vagal innervation of the entire viscera including a hypothetical vagal sensory or motor innervation of the spleen, did not reduce the protective effect of vagal afferent stimulation against AKI. One possible explanation is that the vagovagal reflex activated by optogenetic stimulation of the vagal sensory afferents does not recruit the subpopulation of vagal efferents responsible for anti-inflammatory effects. Alternately, sympathetic efferents and vagal efferents may contribute to the protection in a redundant manner, where eliminating one of them does not cancel the protection due to compensation. Thus, the contribution of a vagovagal reflex to kidney protection is not completely excluded. Nevertheless, subdiaphragmatic vagotomy data clearly indicate that there is a pathway other than vagal efferents, and the importance of the sympathetic system was demonstrated both pharmacologically (ganglionic blockade) and by denervating the spleen. Although vagal afferent stimulation activates other sympathetic nerves, the splenic nerve was of critical importance as shown by the inefficacy of adrenal gland removal or renal denervation.

Next, we sought to identify a central node in the CNS that mediates the vagosympathetic splenic reflex to confer kidney protection. The C1 neurons, which reside in the medulla oblongata, are activated by various physical stressors and circulating inflammatory molecules and regulate both divisions of the autonomic nervous system and the HPA axis (36, 37). Selective stimulation of C1 neurons protects the kidneys from AKI, and a brief restraint stress, which also protects the kidneys, requires the integrity of the C1 neurons (38). As shown here, C1 neurons are also activated by vagus afferent fiber stimulation and their presence is necessary for the kidney protection by vagus afferent fiber stimulation. Thus, C1 neurons appear to mediate the renal protection elicited by vagal afferent stimulation as well as by acute stress. A direct connection between C1 neurons and spleen-regulating sympathetic preganglionic neurons is the most plausible pathway. However, neurons expressing corticotropin-releasing hormone located in the central nucleus of the amygdala and the hypothalamic paraventricular nucleus regulate the formation of splenic plasma cells and adaptive immunity also by activating the splenic nerve (54). These nuclei receive a heavy input from C1 neurons (55) and could partly mediate the splenic nerve activation,

hence the protection against kidney injury elicited by vagal afferent stimulation.

Bilateral kidney IRI per se can activate C1 neurons (56). Thus, it is possible that injured kidneys send a danger signal to C1 neurons possibly via vagal or somatic afferent neurons and elicit the protective pathway ending at the kidneys, forming the kidney–brain reflex pathway, and that VNS or restraint stress potentially augments this suboptimally stimulated self-alleviating reflex pathway. The methods employed in our current study now make it feasible to test the significance of this hypothetical reflex pathway and whether the protective neural circuit involving afferent vagus nerve and C1 neurons is effective in other diseases or conditions.

The identified neural circuit (starting from vagus afferent fibers and subsequently activating the splenic nerve) in the protection against AKI that we observed in mice has not yet been demonstrated in humans. However, a recent pilot study showed that noninvasive transcutaneous stimulation of the auricular branch of the vagus (sensory afferent fibers) attenuated disease severity in patients with rheumatoid arthritis, suggesting that vagus afferent fiber stimulation is also effective in humans (57). This is very important because it provides a noninvasive alternative to cervical VNS, which requires an invasive surgery to implant a device in the neck and chest, and because anti-inflammatory effects of cervical VNS have been attributed to the stimulation of vagus efferent fibers. Our study demonstrates that selective vagus afferent fiber stimulation is effective in kidney protection and requires the integrity of the sympathetic nervous system and the spleen to exert a protective effect against AKI. Our study suggests that auricular VNS might also be effective in kidney protection. Auricular VNS remains to be further explored by clinical trials as a protective pretreatment to patients who are at risk for AKI, such as in cardiac surgery and kidney transplantation, and our study provides important information in designing such clinical trials.

In summary, this is a study of optogenetic stimulation of the vagus nerve to distinguish anterograde versus retrograde stimulation in efferent versus afferent fibers. We found that two distinct neural pathways contribute to the protection against AKI by electrical VNS: anterograde efferent fiber stimulation and anterograde afferent fiber stimulation. We further identified the C1 neurons–sympathetic nervous system–splenic nerve–spleen–kidney axis as the downstream pathway of anterograde vagus afferent fiber stimulation. Our data provide a map of the neural circuits important for kidney protection induced by VNS.

Materials and Methods

Study Design. Detailed methods can be found in *SI Appendix*.

VNS and Miscellaneous Recordings in Mice. For optogenetic and electrical VNS, all mice were anesthetized with an intraperitoneal (i.p.) injection of ketamine (120 mg/kg) and xylazine (12 mg/kg). Depth of anesthesia was assessed by absence of the corneal and hindpaw withdrawal reflexes. Additional anesthetic was administered as necessary (10% of the original dose, i.p.). Body temperature was maintained at 37.0 ± 0.5 °C with a servo-controlled temperature pad (TC-1000; CWE). We stimulated the left cervical vagus nerve because this nerve is usually selected for stimulation in animals and humans (24, 58, 59). The left cervical vagus nerve was isolated via a

Tanaka et al.
Vagus nerve stimulation activates two distinct neuroimmune circuits converging in the spleen to protect mice from kidney injury

PNAS | 9 of 12
https://doi.org/10.1073/pnas.2021758118

www.manaraa.com

midline cervical incision. For optogenetic VNS with *Chat-ChR2* mice and *Vglut2-ChR2* mice, an optic fiber (200 μm core, Thorlabs) coupled to a diode-pumped solid-state laser light source (473 nm, 50 mW, Shanghai Laser & Optics Century) was positioned for focal illumination. Laser application (10 ms pulses, ~280 mW/mm² intensity; for physiological experiments: 1 to 20 Hz for 10 s; for kidney IRI experiments: 5 Hz for 10 min) was controlled by Spike 2 software (v7.06; CED). Sham operation was done by setting the laser output to zero for the experiments to measure plasma corticosterone (Fig. 4*A*) or was done by delivering the same trains of laser light (10 ms pulses, ~280 mW/mm² intensity, 5 Hz for 10 min) to Cre-negative littermates for the other experiments. In a subset of *Chat-ChR2* mice and *Vglut2-ChR2* mice, an optic fiber was positioned at the distal or central end of the transected vagus nerve or at the distal or central side of the area anesthetized with bupivacaine (2.5 mg/mL), a local anesthetic, to distinguish anterograde versus retrograde stimulation in efferent or afferent fibers. For bupivacaine application, a small piece of gauze soaked with bupivacaine was wrapped around the vagus nerve. In another subset of *Vglut2-ChR2* and control mice, drugs were given i.p. 30 min before optogenetic VNS (30 mg/kg hexamethonium bromide, a ganglionic blocker or 30 mg/kg mifepristone, a corticosterone receptor antagonist). Electrical VNS in wild-type mice (square wave, 5 Hz, 50 μA intensity, 1 ms pulses) was performed for 10 min using a bipolar silver wire electrode (AS633; Cooner Wire), Grass model S88 stimulator, and stimulus isolation unit (Astro-Med Inc.). In sham-operated animals, vagus nerve was isolated but not stimulated. For electrical (distal or central) VNS in *Dbh-Cre* mice, bupivacaine (2.5 mg/mL) was applied to the isolated vagus nerve to block nerve conduction, and a bipolar silver wire electrode was placed at the distal or central side of the anesthetized area. In sham-operated animals, vagus nerve was treated with bupivacaine but not stimulated. The parameters for electrical VNS were determined in our previous work (24) in which stimulation with those parameters produced a small but significant decrease in heart rate without a decrease in blood pressure.

Heart rate was recorded using ECG electrodes (lead II) inserted subcutaneously (s.c.). Respiratory rate was measured by capnography (Micro-Capnograph CI240, Columbus Instruments). In a subset of *Chat-ChR2*, *Vglut2-ChR2*, and control mice, the left vagus nerve was placed on a bipolar stainless-steel electrode (AS633; Cooner Wire) to record evoked action potentials during blue laser application to the same nerve. Electrodes and nerves were then embedded in silicone (Kwik-Sil, World Precision Instruments). Physiological signals were filtered and amplified (30 to 3,000 Hz, x10,000; BMA-400 amplifier, CWE). The analog signals were digitized (Micro3 1401; CED) and processed using Spike 2 software (v7.06; CED). Recording of sympathetic nerve activity in rats is described in a separate section below.

Kidney IRI in Mice. Twenty-four hours after VNS or sham treatments, mice were anesthetized with an i.p. injection of ketamine (120 mg/kg) and xylazine (12 mg/kg) and underwent bilateral kidney IRI, as described (60). Briefly, bilateral kidney IRI was performed through flank incisions by clamping the renal pedicles for 26 min. The clamps were then removed, and the wound was sutured after restoration of blood flow was visually observed. Sham-operated mice underwent the same procedure except that the renal pedicles were not clamped. Mice received buprenorphine SR (0.5 mg/kg) as a postoperative analgesic. Kidneys were allowed to reperfuse for a period of 24 h. This surgical procedure was conducted blind (i.e., the person performing the renal clamp had no knowledge of experimental setting including genotype). Twenty-four hours after the surgery, the mice were euthanized with an overdose of ketamine and xylazine, and blood (400 to 600 μL) was collected from the retroorbital sinus. The kidneys were harvested for histology and RNA extraction. In some experiments, mice were perfused with fixative, and the brain was collected for histology (see sections on brain histology for details).

Plasma Creatinine, Cytokine Measurement, Renal Histology, and Real-Time PCR. Detailed methods can be found in *SI Appendix*.

Effect of Vagus Afferent/Efferent Fiber Stimulation on the Activation of C1 Neurons. To investigate whether C1 neurons are activated by vagus afferent fiber stimulation, the left cervical vagus nerve was exposed and illuminated with blue laser for 10 min (5 Hz), as described above, in control, *Vglut2-ChR2*, and *Chat-ChR2* mice. After 90 min, the mice were perfused with fixative, and the brain was collected for histology (see the brain histology section for details). c-Fos immunoreactivity (in nuclei) was used as a marker of neuron activation (61), and TH immunoreactivity (in cytoplasm) was used to identify C1 neurons, which are the only neurons in the RVLM that are positive for TH (see section on brain histology for details). TH⁺ cells (all C1 neurons) and TH⁺c-Fos⁺ cells (activated C1 neurons) were counted in bilateral RVLM (see section on brain histology for details), and the fraction of activated C1 neurons was calculated in each animal.

Brain Histology. Mice were euthanized with an overdose of ketamine and xylazine and perfused transcardially with 50 mL of heparinized saline followed by 100 mL of freshly prepared 4% paraformaldehyde in sodium phosphate buffer (pH 7.4). Brains were extracted and postfixed at 4 °C for 24 to 48 h in the same fixative. Transverse sections (30 μm thick) were cut on a vibrating microtome and stored in a cryoprotectant solution (20% glycerol, 30% ethylene glycol, 50% 100 mM phosphate buffer, pH 7.4) at −20 °C. Immunohistochemical and in situ hybridization procedures and microscopy were performed as previously described (38). The following antibodies were used: TH was detected with a sheep polyclonal antibody (1:1,000; Millipore #AB1542; EMD Millipore) followed by Alexa Fluor 647-tagged donkey anti-sheep IgG (1:500; Jackson ImmunoResearch Laboratories) or by Alexa Fluor 488-tagged donkey anti-sheep IgG (1:500; Jackson ImmunoResearch Laboratories); c-Fos protein was detected with a rabbit polyclonal antibody (1:10,000; #226 003; Synaptic Systems) followed by Cy3-tagged donkey anti-rabbit IgG (1:500; Jackson ImmunoResearch Laboratories); mCherry protein was detected with anti-DsRed (rabbit polyclonal, 1:1,000; #632496; Clontech Laboratories) followed by Cy3-tagged donkey anti-rabbit IgG (1:500; Jackson ImmunoResearch Laboratories); ChR2-eYFP was detected with a chicken polyclonal antibody (1:1,000; #GFP-1020; Aves Labs) followed by Alexa Fluor 488-tagged donkey anti-chicken IgY (1:500; Jackson ImmunoResearch Laboratories); ChAT was detected with a goat polyclonal antibody (1:100; Millipore #AB144P; EMD Millipore) followed by Alexa Fluor 647-tagged donkey anti-goat IgG (1:500; Jackson ImmunoResearch Laboratories). *Vglut2* mRNA was detected by in situ hybridization (probe for mouse *Vglut2*: #319171, Amplification kit: #320851, Protease kit: #322340; Advanced Cell Diagnostics) as per the manufacturer's protocol.

Brain sections were examined under brightfield and epifluorescence illumination with a Zeiss AxioImager Z.1 microscope equipped with a computer-controlled stage and Neurolucida software (Version 11; MBF Bioscience). The same system was also used to directly observe ChR2-eYFP signal in the left cervical vagus nerve and nodose ganglion of control, *Vglut2-ChR2*, and *Chat-ChR2* mice. An investigator blinded to the experimental identity of the sections performed cell counts in a 1-in-3 series of sections of brainstem that were kept in correct sequential order. Sections from different mice were aligned according to their distance from a reference transverse plane identified as 6.48 mm caudal to bregma, after Paxinos and Franklin (62). The plane of this section intersects the most caudal portion of the facial motor nucleus. Images were obtained with a Zeiss MRc camera as TIFF files. For representative images, TH and c-Fos/mCherry were shown in green and magenta, respectively. The area positive for both TH and mCherry appears in white. Pseudo colors were used as necessary. Output levels were adjusted to include all information-containing pixels. Balance and contrast were adjusted to reflect true rendering as much as possible. No other image retouching was performed.

Viral Vectors. AAV-DIO-EF1α-mCherry serotype 2 (AAV2-mCherry; control vector) and AAV2-DIO-taCasp3-TEVp were purchased from the University of North Carolina vector core (the first construct courtesy of K. Deisseroth [Stanford University] and second construct courtesy of N. Shah [University of San Francisco]). In these vectors, the mCherry and taCasp3-TEVp sequences are flanked by the same double-lox sites (LoxP and lox2722).

Injections of Viral Vector into the RVLM. AAV2-DIO-taCasp3-TEVp and AAV2-mCherry (control vector) were injected bilaterally into the RVLM. The injections were made under aseptic conditions in mice anesthetized with a mixture of ketamine (100 mg/kg) and dexmedetomidine (0.2 mg/kg; i.p.). Depth of anesthesia was deemed sufficient if the corneal and hindpaw withdrawal reflexes were absent. Additional anesthetic was administered as necessary (10% of the original dose, i.p.). Body temperature was maintained at 37.0 ± 0.5 °C with a servo-controlled temperature pad (TC-1000; CWE). The mandibular branch of the facial nerve was revealed through a small skin incision (left side or both sides as required) for later electrical stimulation. The mice were then placed prone on a Kopf 1730 stereotaxic apparatus adapted for mouse stereotaxic injections (ear bar adaptor, model EB-5N; Narishige Scientific Instrument Lab; bite bar, Model 926 mouse adaptor set at −2 mm; David Kopf Instruments). The viral vector was loaded into a glass pipette with a 1.2 mm internal diameter, broken to a 25 μm tip (external diameter), and introduced into the brain through a 1.5 mm diameter hole that was drilled into the occipital plate caudal to the parieto-occipital suture on both sides. The facial nerve was stimulated (0.1 ms, 1 to 300 μA, 1 Hz) to evoke antidromic field potentials within the facial motor nucleus (55). These field potentials, recorded via the vector-filled pipette, were used to map the caudal end of the facial motor nucleus and thus identify the location of C1 neurons that reside immediately caudal to this nucleus. For bilateral administration of vector, three 140 nL injections were made 300 μm above the base of the medulla oblongata (determined as the lower limit of the

Tanaka et al.
Vagus nerve stimulation activates two distinct neuroimmune circuits converging in the
spleen to protect the kidney from ischemia–reperfusion injury

facial field potential) and at the medial edge of the respiratory column (identified by respiratory synchronous multiunit activity) on each side. The three injections were separated by 200 μm and were aligned rostrocaudally. Sham-operated mice underwent the same procedure, except the injections were not performed. Mice received postoperative boluses of atipamezole (α_2 adrenergic antagonist, 2 mg/kg, s.c.), ampicillin (125 mg/kg, i.p.), and ketoprofen (4 mg/kg, s.c.). Ampicillin and ketoprofen were readministered 24 h postoperatively. Mice were housed in the University of Virginia vivarium for at least 5 wk after virus injection before performing electrical VNS and kidney IRI. Mice were maintained in groups of 3 to 5 per cage on a 12:12 h light:dark cycle. During this time, mice gained weight normally and appeared unperturbed. These mice were randomly divided into the various treatment groups. The efficacy of C1 ablation was confirmed by counting TH⁺ cells in bilateral RVLM (all TH⁺ cells in RVLM are C1 neurons) in each animal (see the brain histology section for details).

Plasma Corticosterone Measurement. To investigate whether the HPA axis is activated by vagus afferent fiber stimulation, *Vglut2-ChR2* mice underwent optogenetic VNS at 5 Hz for 10 min as described above. In a subset of *Vglut2-ChR2* mice, an optic fiber was positioned at the distal or central side of the area anesthetized with bupivacaine for retrograde or anterograde stimulation, respectively. Sham operation was done by setting the laser output to zero with ("Bupivacaine only" group) or without ("Sham" group) bupivacaine application. Blood (400 to 600 μL; final EDTA concentration: 0.1%) was collected by cardiac puncture immediately after VNS. Plasma was prepared by centrifuging blood at 1,000 g for 15 min at 4 °C and stored at −80 °C until analysis. All of these experiments were conducted between 1 and 5 PM. Corticosterone was measured by radioimmunoassay at the Vanderbilt Hormone Assay & Analytical Services Core in a blinded fashion.

Subdiaphragmatic Vagotomy. Mice were anesthetized with an i.p. injection of ketamine (120 mg/kg) and xylazine (12 mg/kg). Depth of anesthesia was assessed by absence of the corneal and hindpaw withdrawal reflexes. Additional anesthetic was administered as necessary (10% of the original dose, i.p.). Body temperature was maintained at 37.0 ± 0.5 °C with a servo-controlled temperature pad (TC-1000; CWE). After middle upper laparotomy, the stomach was gently manipulated to expose the esophagus. Then, both anterior and posterior trunks of the vagus nerve were identified between the diaphragm and the gastric cardia and transected. Mice received boluses of ampicillin (125 mg/kg, i.p.) and ketoprofen (4 mg/kg, sc) immediately after surgery and again 24 h later. Four additional mice were used to test the efficacy of the vagotomy procedure. Two mice were subjected to subdiaphragmatic vagotomy and the rest underwent sham surgery, in which the abdominal vagus nerves were similarly exposed but not cut. Seven days after surgery, the mice received an i.p. injection of 200 μL of Fluoro-Gold. After four days, the mice were deeply anesthetized and perfused with fixative (as described in the section on brain histology). Brains were removed and postfixed in 4% paraformaldehyde for up to three days, and then all brains were sectioned as described above.

Adrenalectomy. To investigate the possibility that catecholamine release from the adrenal medulla contributes to the kidney protection by afferent VNS, bilateral adrenalectomy was performed in *Vglut2-ChR2* and control mice seven days before optogenetic VNS. The mice were anesthetized with an i.p. injection of ketamine (120 mg/kg) and xylazine (12 mg/kg). Depth of anesthesia was assessed by absence of the corneal and hindpaw withdrawal reflexes. Additional anesthetic was administered as necessary (10% of the original dose, i.p.). Body temperature was maintained at 37.0 ± 0.5 °C with a servo-controlled temperature pad (TC-1000; CWE). After middle laparotomy, the adrenal gland on each side was exposed and the entire adrenal gland was removed. Mice received buprenorphine-SR (0.5 mg/kg) as a postoperative analgesic. Since the adrenal gland releases not only catecholamines (from the medulla) but also corticosterone and aldosterone (from the cortex), adrenalectomized mice were given dexamethasone [12 μg/kg/d, s.c., 3 d/wk (63, 64)], and drinking water was replaced with 0.9% NaCl.

Splenic and Renal Nerve Denervation. Splenic nerve denervation and bilateral renal nerve denervation were performed under anesthesia (ketamine [120 mg/kg] and xylazine [12 mg/kg]). Depth of anesthesia was assessed by absence of the corneal and hindpaw withdrawal reflexes. Additional anesthetic was administered as necessary (10% of the original dose, i.p.). Body temperature was maintained at 37.0 ± 0.5 °C with a servo-controlled temperature pad (TC-1000; CWE). The renal vessels or branches of splenic vessels were identified through flank incisions, stripped of nerves and connective tissue, and encircled with a 5-0 suture soaked with 10% phenol in ethanol, a process that ablates the

coexistent nerves (65, 66). In sham-operated mice, the stripping procedure was not performed, and normal saline was applied instead of phenol. Then the denervation site was vigorously washed with normal saline. Mice received buprenorphine-SR (0.5 mg/kg) as a postoperative analgesic. Seven days after denervation surgery, mice were euthanized to confirm the efficacy and selectivity of denervation by evaluating TH immunohistochemistry (described in the renal histology section) and norepinephrine levels (described below) in the spleen and kidney, or they underwent optogenetic VNS and kidney IRI. The renal denervation protocol was optimized so that the denervation per se was not protective against kidney IRI (24).

Norepinephrine Measurement in the Spleen and Kidney. The spleen and kidney were removed seven days after denervation, snap frozen in liquid nitrogen, and ground to a powder with mortars and pestles chilled in liquid nitrogen. Glutathione/perchloric acid solution (5 mM reduced glutathione in 0.4 N perchloric acid) was added to the samples (1 mL/100 mg tissue). After homogenization and centrifugation, supernatant was collected and kept at −80 °C until analysis. Norepinephrine was measured by HPLC at the Vanderbilt Hormone Assay & Analytical Services Core in a blinded fashion (detection limit: 25 pg/mL [0.25 pg/mg tissue]).

Splenectomy. Mice were anesthetized with an i.p. injection of ketamine (120 mg/kg) and xylazine (12 mg/kg). Depth of anesthesia was assessed by absence of the corneal and hindpaw withdrawal reflexes. Additional anesthetic was administered as necessary (10% of the original dose, i.p.). Body temperature was maintained at 37.0 ± 0.5 °C with a servo-controlled temperature pad (TC-1000; CWE). The splenic vasculature was ligated, and the spleen was removed through a left flank incision. Mice received buprenorphine-SR (0.5 mg/kg) as a postoperative analgesic. Splenectomized mice were allowed to recover for seven days prior to optogenetic VNS and IRI studies.

Adoptive Transfer Studies. Spleens, inguinal lymph nodes, and bone marrow were harvested from donor mice 24 h after VNS surgery. Single-cell suspensions were generated by passing the tissues through 40-μm filters into phosphate-buffered saline (PBS), and the cell pellet was collected by centrifugation (500 g for 5 min). Splenocytes were then treated with red blood cell lysis buffer (BioLegend) according to the manufacturer's protocol. The cell pellet was diluted in PBS, and splenocytes (1×10^6 cells/recipient mouse) (24), lymph node cells (1×10^5 or 1×10^6 cells/recipient mouse), or bone marrow cells (1×10^5, 1×10^6, or 1×10^7 cells/recipient mouse) were injected via tail vein 24 h prior to kidney IRI.

Rat Experiments (VNS, Sympathetic Nerve Recordings, and IRI). Detailed methods can be found in *SI Appendix*.

Statistical Analysis. Statistical analyses were performed using GraphPad Prism 8.3.0 software. All data sets were tested for normality using the Shapiro–Wilk test. All values are expressed as mean and SEM. When no error bar is shown, this is because the data were not normally distributed, and a nonparametric test was used. Unpaired two-sided Student's *t* test or two-sided Mann–Whitney test was used for comparisons between two groups. One- or two-way ANOVA followed by the Tukey's or Sidak's test or Kruskal–Wallis followed by Dunn's test was used to compare multiple groups. $P < 0.05$ was considered statistically significant.

Study Approval. All animals were handled and procedures were performed in adherence to the NIH *Guide for the Care and Use of Laboratory Animals*. All protocols were approved by the University of Virginia Institutional Animal Care and Use Committee or the Animal Research Committees of Gifu University.

Data Availability. All study data are included in the article and/or supporting information.

MEDICAL SCIENCES

Tanaka et al.
Vagus nerve stimulation activates two distinct neuroimmune circuits converging in the spleen to protect mice from kidney injury

PNAS | 11 of 12
https://doi.org/10.1073/pnas.2021758118

www.manaraa.com

1. C. Ronco, R. Bellomo, J. A. Kellum, Acute kidney injury. *Lancet* **394**, 1949–1964 (2019).
2. A. S. Levey, M. T. James, Acute kidney injury. *Ann. Intern. Med.* **167**, ITC66–ITC80 (2017).
3. L. S. Chawla, P. W. Eggers, R. A. Star, P. L. Kimmel, Acute kidney injury and chronic kidney disease as interconnected syndromes. *N. Engl. J. Med.* **371**, 58–66 (2014).
4. S. G. Coca, S. Singanamala, C. R. Parikh, Chronic kidney disease after acute kidney injury: A systematic review and meta-analysis. *Kidney Int.* **81**, 442–448 (2012).
5. A. C. Webster, E. V. Nagler, R. L. Morton, P. Masson, Chronic kidney disease. *Lancet* **389**, 1238–1252 (2017).
6. K. U. Eckardt *et al.*, Evolving importance of kidney disease: From subspecialty to global health burden. *Lancet* **382**, 158–169 (2013).
7. "Neuroimmune communication." *Nat. Immunol.* **18**, 115 (2017).
8. "Neuroimmune communication." *Nat. Neurosci.* **20**, 127 (2017).
9. K. J. Tracey, Physiology and immunology of the cholinergic antiinflammatory pathway. *J. Clin. Invest.* **117**, 289–296 (2007).
10. M. Rosas-Ballina *et al.*, Splenic nerve is required for cholinergic antiinflammatory pathway control of TNF in endotoxemia. *Proc. Natl. Acad. Sci. U.S.A.* **105**, 11008–11013 (2008).
11. D. L. Bellinger, S. Y. Felten, D. Lorton, D. L. Felten, Origin of noradrenergic innervation of the spleen in rats. *Brain Behav. Immun.* **3**, 291–311 (1989).
12. H. R. Berthoud, T. L. Powley, Characterization of vagal innervation to the rat celiac, suprarenal and mesenteric ganglia. *J. Auton. Nerv. Syst.* **42**, 153–169 (1993).
13. H. R. Berthoud, T. L. Powley, Interaction between parasympathetic and sympathetic nerves in prevertebral ganglia: Morphological evidence for vagal efferent innervation of ganglion cells in the rat. *Microsc. Res. Tech.* **35**, 80–86 (1996).
14. M. Li, J. Galligan, D. Wang, G. Fink, The effects of celiac ganglionectomy on sympathetic innervation to the splanchnic organs in the rat. *Auton. Neurosci.* **154**, 66–73 (2010).
15. D. M. Nance, J. Burns, Innervation of the spleen in the rat: Evidence for absence of afferent innervation. *Brain Behav. Immun.* **3**, 281–290 (1989).
16. M. Rosas-Ballina *et al.*, Acetylcholine-synthesizing T cells relay neural signals in a vagus nerve circuit. *Science* **334**, 98–101 (2011).
17. H. Wang *et al.*, Nicotinic acetylcholine receptor alpha7 subunit is an essential regulator of inflammation. *Nature* **421**, 384–388 (2003).
18. E. Meroni *et al.*, Functional characterization of oxazolone-induced colitis and survival improvement by vagus nerve stimulation. *PLoS One* **13**, e0197487 (2018).
19. G. Matteoli *et al.*, A distinct vagal anti-inflammatory pathway modulates intestinal muscularis resident macrophages independent of the spleen. *Gut* **63**, 938–948 (2014).
20. G. S. Bassi *et al.*, Modulation of experimental arthritis by vagal sensory and central brain stimulation. *Brain Behav. Immun.* **64**, 330–343 (2017).
21. E. N. Komegae *et al.*, Vagal afferent activation suppresses systemic inflammation via the splanchnic anti-inflammatory pathway. *Brain Behav. Immun.* **73**, 441–449 (2018).
22. S. Hoeger *et al.*, Modulation of brain dead induced inflammation by vagus nerve stimulation. *Am. J. Transplant.* **10**, 477–489 (2010).
23. S. Hoeger *et al.*, Vagal stimulation in brain dead donor rats decreases chronic allograft nephropathy in recipients. *Nephrol. Dial. Transplant.* **29**, 544–549 (2014).
24. T. Inoue *et al.*, Vagus nerve stimulation mediates protection from kidney ischemia-reperfusion injury through α7nAChR+ splenocytes. *J. Clin. Invest.* **126**, 1939–1952 (2016).
25. E. K. Williams *et al.*, Sensory neurons that detect stretch and nutrients in the digestive system. *Cell* **166**, 209–221 (2016).
26. R. B. Chang, D. E. Strochlic, E. K. Williams, B. D. Umans, S. D. Liberles, Vagal sensory neuron subtypes that differentially control breathing. *Cell* **161**, 622–633 (2015).
27. S. S. Chavan, V. A. Pavlov, K. J. Tracey, Mechanisms and therapeutic relevance of neuro-immune communication. *Immunity* **46**, 927–942 (2017).
28. J. E. Choi, A. Di Nardo, Skin neurogenic inflammation. *Semin. Immunopathol.* **40**, 249–259 (2018).
29. P. Baral *et al.*, Nociceptor sensory neurons suppress neutrophil and γδ T cell responses in bacterial lung infections and lethal pneumonia. *Nat. Med.* **24**, 417–426 (2018).
30. I. M. Chiu *et al.*, Bacteria activate sensory neurons that modulate pain and inflammation. *Nature* **501**, 52–57 (2013).
31. F. A. Pinho-Ribeiro *et al.*, Blocking neuronal signaling to immune cells treats streptococcal invasive infection. *Cell* **173**, 1083–1097.e22 (2018).
32. L. E. Goehler *et al.*, Vagal immune-to-brain communication: A visceral chemosensory pathway. *Auton. Neurosci.* **85**, 49–59 (2000).
33. C. J. Padro, V. M. Sanders, Neuroendocrine regulation of inflammation. *Semin. Immunol.* **26**, 357–368 (2014).
34. D. W. Cain, J. A. Cidlowski, Immune regulation by glucocorticoids. *Nat. Rev. Immunol.* **17**, 233–247 (2017).
35. S. A. Aicher *et al.*, Monosynaptic projections from the nucleus tractus solitarii to C1 adrenergic neurons in the rostral ventrolateral medulla: Comparison with input from the caudal ventrolateral medulla. *J. Comp. Neurol.* **373**, 62–75 (1996).
36. P. G. Guyenet *et al.*, C1 neurons: The body's EMTs. *Am. J. Physiol. Regul. Integr. Comp. Physiol.* **305**, R187–R204 (2013).
37. H. Y. Li, A. Ericsson, P. E. Sawchenko, Distinct mechanisms underlie activation of hypothalamic neurosecretory neurons and their medullary catecholaminergic afferents in categorically different stress paradigms. *Proc. Natl. Acad. Sci. U.S.A.* **93**, 2359–2364 (1996).
38. C. Abe *et al.*, C1 neurons mediate a stress-induced anti-inflammatory reflex in mice. *Nat. Neurosci.* **20**, 700–707 (2017).
39. L. Vong *et al.*, Leptin action on GABAergic neurons prevents obesity and reduces inhibitory tone to POMC neurons. *Neuron* **71**, 142–154 (2011).
40. J. Rossi *et al.*, Melanocortin-4 receptors expressed by cholinergic neurons regulate energy balance and glucose homeostasis. *Cell Metab.* **13**, 195–204 (2011).
41. H. Xie *et al.*, Therapeutic potential of α7 nicotinic acetylcholine receptor agonists to combat obesity, diabetes, and inflammation. *Rev. Endocr. Metab. Disord.* **21**, 431–447 (2020).
42. M. K. Sun, P. G. Guyenet, Arterial baroreceptor and vagal inputs to sympathoexcitatory neurons in rat medulla. *Am. J. Physiol.* **252**, R699–R709 (1987).
43. T. J. Rosol, J. T. Yarrington, J. Latendresse, C. C. Capen, Adrenal gland: Structure, function, and mechanisms of toxicity. *Toxicol. Pathol.* **29**, 41–48 (2001).
44. D. B. Bylund *et al.*, International union of pharmacology nomenclature of adrenoceptors. *Pharmacol. Rev.* **46**, 121–136 (1994).
45. C. F. Yang *et al.*, Sexually dimorphic neurons in the ventromedial hypothalamus govern mating in both sexes and aggression in males. *Cell* **153**, 896–909 (2013).
46. F. A. Koopman *et al.*, Vagus nerve stimulation inhibits cytokine production and attenuates disease severity in rheumatoid arthritis. *Proc. Natl. Acad. Sci. U.S.A.* **113**, 8284–8289 (2016).
47. B. Bonaz *et al.*, Chronic vagus nerve stimulation in Crohn's disease: A 6-month follow-up pilot study. *Neurogastroenterol. Motil.* **28**, 948–953 (2016).
48. L. V. Borovikova *et al.*, Vagus nerve stimulation attenuates the systemic inflammatory response to endotoxin. *Nature* **405**, 458–462 (2000).
49. P. S. Olofsson *et al.*, Single-pulse and unidirectional electrical activation of the cervical vagus nerve reduces tumor necrosis factor in endotoxemia. *Bioelectron. Med.* **2**, 37 (2015).
50. B. O. Bratton *et al.*, Neural regulation of inflammation: No neural connection from the vagus to splenic sympathetic neurons. *Exp. Physiol.* **97**, 1180–1185 (2012).
51. D. Martelli, M. J. McKinley, R. M. McAllen, The cholinergic anti-inflammatory pathway: A critical review. *Auton. Neurosci.* **182**, 65–69 (2014).
52. G. Cano, A. F. Sved, L. Rinaman, B. S. Rabin, J. P. Card, Characterization of the central nervous system innervation of the rat spleen using viral transneuronal tracing. *J. Comp. Neurol.* **439**, 1–18 (2001).
53. S. Kumar *et al.*, Dexamethasone ameliorates renal ischemia-reperfusion injury. *J. Am. Soc. Nephrol.* **20**, 2412–2425 (2009).
54. X. Zhang *et al.*, Brain control of humoral immune responses amenable to behavioural modulation. *Nature* **581**, 204–208 (2020).
55. S. B. Abbott *et al.*, Selective optogenetic activation of rostral ventrolateral medullary catecholaminergic neurons produces cardiorespiratory stimulation in conscious mice. *J. Neurosci.* **33**, 3164–3177 (2013).
56. W. Cao *et al.*, Reno-cerebral reflex activates the renin-angiotensin system, promoting oxidative stress and renal damage after ischemia-reperfusion injury. *Antioxid. Redox Signal.* **27**, 415–432 (2017).
57. M. E. Addorisio *et al.*, Investigational treatment of rheumatoid arthritis with a vibrotactile device applied to the external ear. *Bioelectron. Med.* **5**, 4 (2019).
58. W. C. Stacey, B. Litt, Technology insight: Neuroengineering and epilepsy-designing devices for seizure control. *Nat. Clin. Pract. Neurol.* **4**, 190–201 (2008).
59. Y. A. Levine *et al.*, Neurostimulation of the cholinergic anti-inflammatory pathway ameliorates disease in rat collagen-induced arthritis. *PLoS One* **9**, e104530 (2014).
60. J. C. Gigliotti *et al.*, Ultrasound prevents renal ischemia-reperfusion injury by stimulating the splenic cholinergic anti-inflammatory pathway. *J. Am. Soc. Nephrol.* **24**, 1451–1460 (2013).
61. J. I. Morgan, D. R. Cohen, J. L. Hempstead, T. Curran, Mapping patterns of c-fos expression in the central nervous system after seizure. *Science* **237**, 192–197 (1987).
62. G. Paxinos, K. B. Franklin, *Paxinos and Franklin's the Mouse Brain in Stereotaxic Coordinates* (Academic Press, 2013).
63. S. D. Crowley *et al.*, Distinct roles for the kidney and systemic tissues in blood pressure regulation by the renin-angiotensin system. *J. Clin. Invest.* **115**, 1092–1099 (2005).
64. T. H. Kwon *et al.*, Regulation of collecting duct AQP3 expression: Response to mineralocorticoid. *Am. J. Physiol. Renal Physiol.* **283**, F1403–F1421 (2002).
65. L. Xiao *et al.*, Renal denervation prevents immune cell activation and renal inflammation in angiotensin II-induced hypertension. *Circ. Res.* **117**, 547–557 (2015).
66. J. Ong *et al.*, Renal sensory nerves increase sympathetic nerve activity and blood pressure in 2-kidney 1-clip hypertensive mice. *J. Neurophysiol.* **122**, 358–367 (2019).

Tanaka et al.
Vagus nerve stimulation activates two distinct neuroimmune circuits converging in the spleen to protect mice from kidney injury